X-raying the wind of the B0 supergiant QV Nor

J. M. Torrejón, N. S. Schulz, M. A. Nowak, L. Oskinova, J.J. Rodes, T. Shenar, J. Wilms

The Universe in High Resolution X-ray Spectra, August 2015, Cambridge MA

Intro

- The **clumpy wind** paradigm in massive stars **well established** (Lucy & Solomon 1980, Owocki et al. 1988, Feldmeir et al. 1997)
- There is, however, **considerable uncertainty on the physical properties of these clumps** (size, density, distribution).
- Of particular interest is the **radial onset of clumping** in the wind of the massive star. Feldmeier et al. 1997 predicted a **smooth widn up to 1.5R$_*$** after which the instabilities develop and fragment the wind.

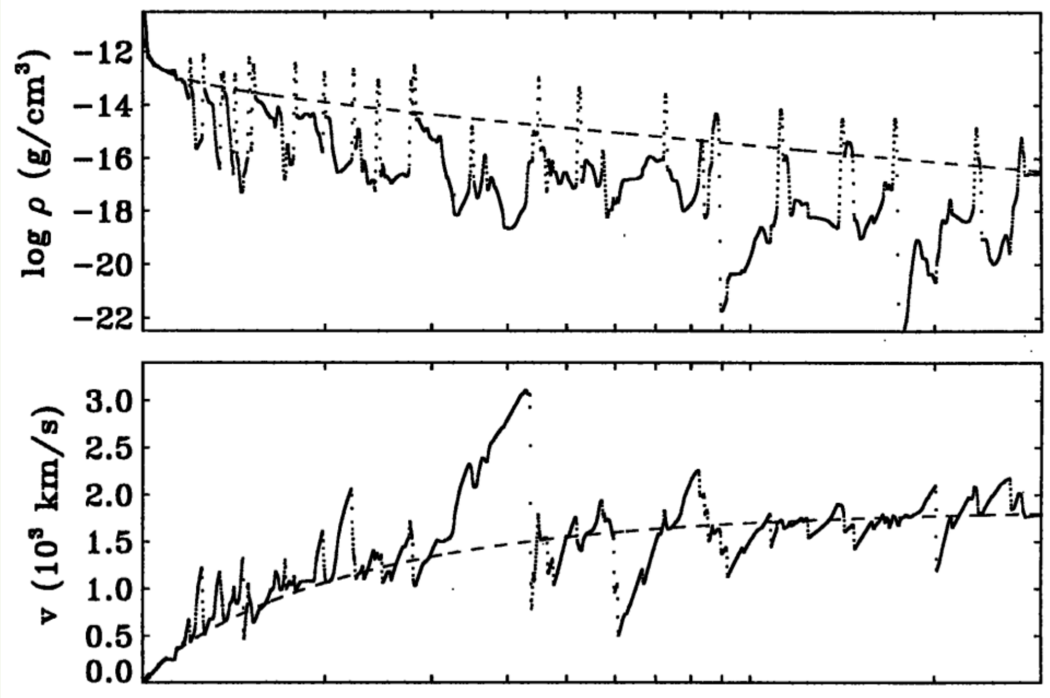

- Observations suggest that the innermost wind regions could be already clumped (Puls et al. 2006, Waldron & Cassinelli 2007).
- Some theoretical models predict **subsurface convection cells in OB stars** (Cantiello & Braithwaite 2011)

Intro.

- In HMXBs a compact object is deeply embeded into the massive star wind providing a source of intense X-ray illumination.

- The X-rays excite transitions in the wind governed by the ionization parameter

$$\xi = Lx/[n(r_x)r_x^2]$$

- The Fe Kα line is regularly observed in virtually all HMXBs (Torrejón et al. 2010, Gimenez-García et al. 2015).

- In order to have strong lines from near-neutral Fe, $\xi \leq 10^2$. For typical luminosities of $Lx \sim 10^{36}$ erg s^{-1} and distances $r_x \sim 10^{11-12}$ cm the required $n \sim 10^{10-12}$ cm^{-3} which is a factor **between 1 and 100 the average wind densities predicted by the smooth wind** scenario.

- **The Fe Kα line is a tracer of the wind "overdensities", i.e., the clumps**.

QV Nor

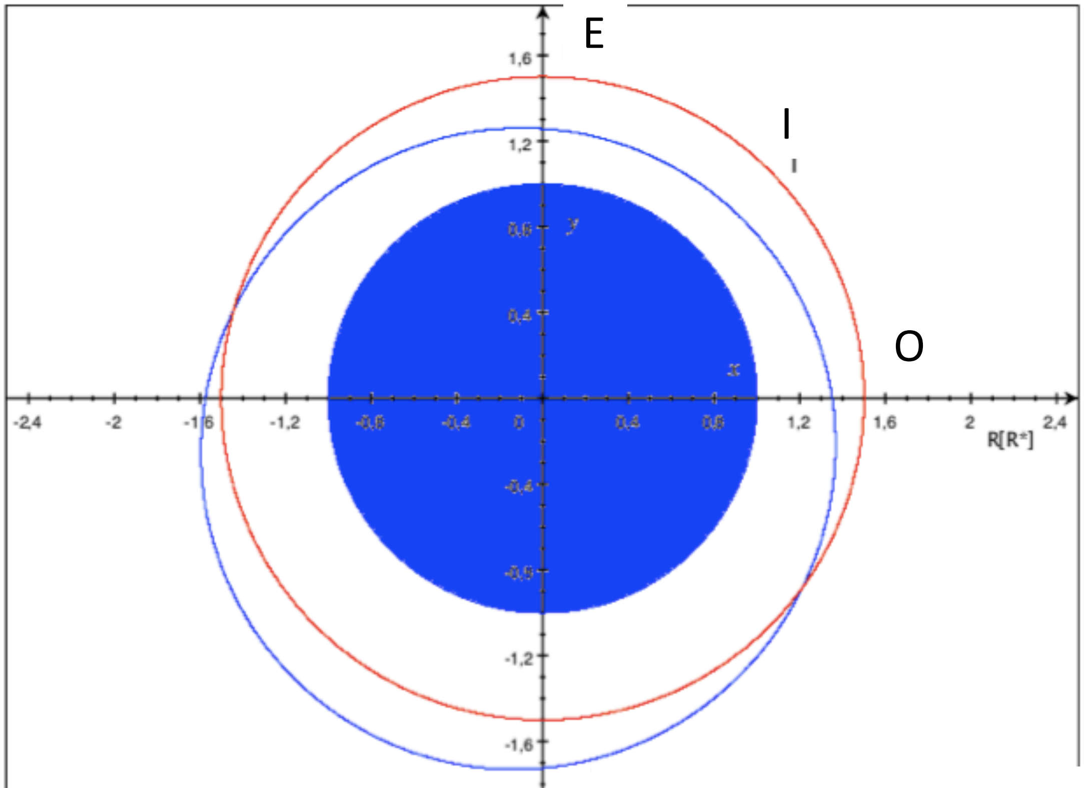

B0 I (supergiant) donor of the X-ray pulsar 4U1538-52. The NS orbits QV Nor every 3.7d

Two orbitial solutions individually **precisally determined** (Clark 2000). The NS at r=[1.2, 1.5]R_* **probing the innermost wind region**.

Wind radial density profile well established (Clark+ 1994=CWN94)

Eclipsing

Periastron passage close to eclipse allowing maximum constrast

HETG Observations journal

ObsID	Date	t_{exp} (ks)	ϕ (start)
15704	2014-02-03 10:27:14	25.63	0.97
16581	2014-02-06 10:21:40	52.27	0.77

HETG Lightcurve

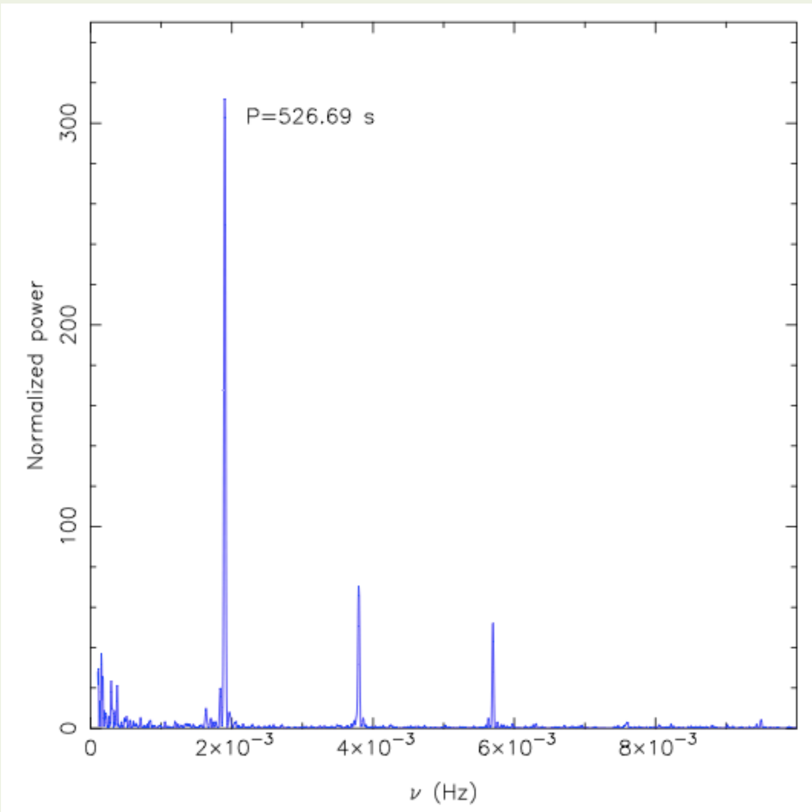

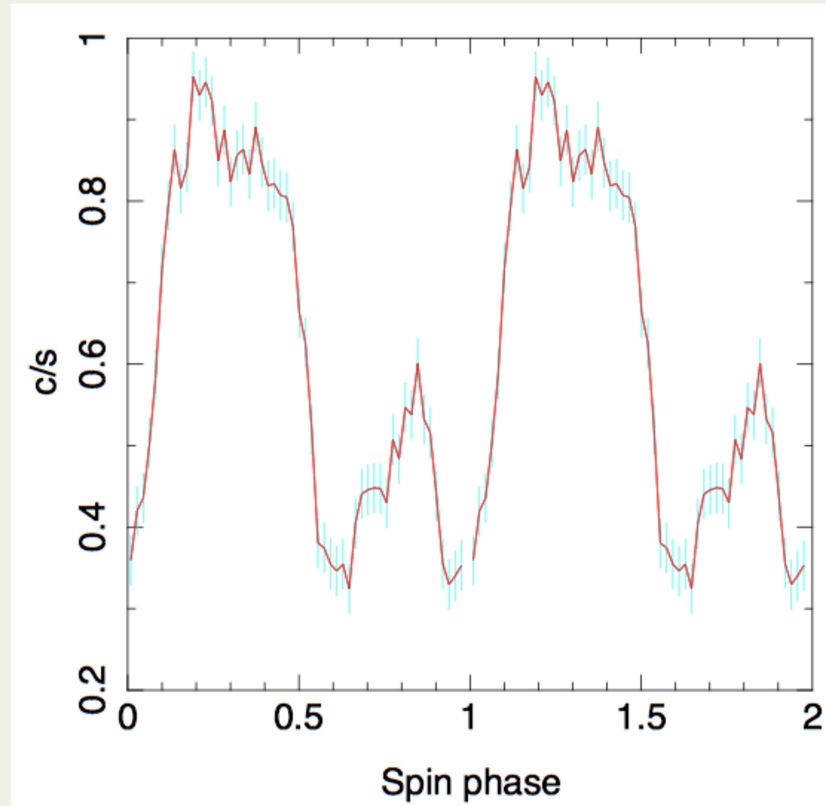

P_{spin} = 526.69 ± 1.31 s

NS Spin pulse

Pulsed fraction 54%

HETG Lightcurve

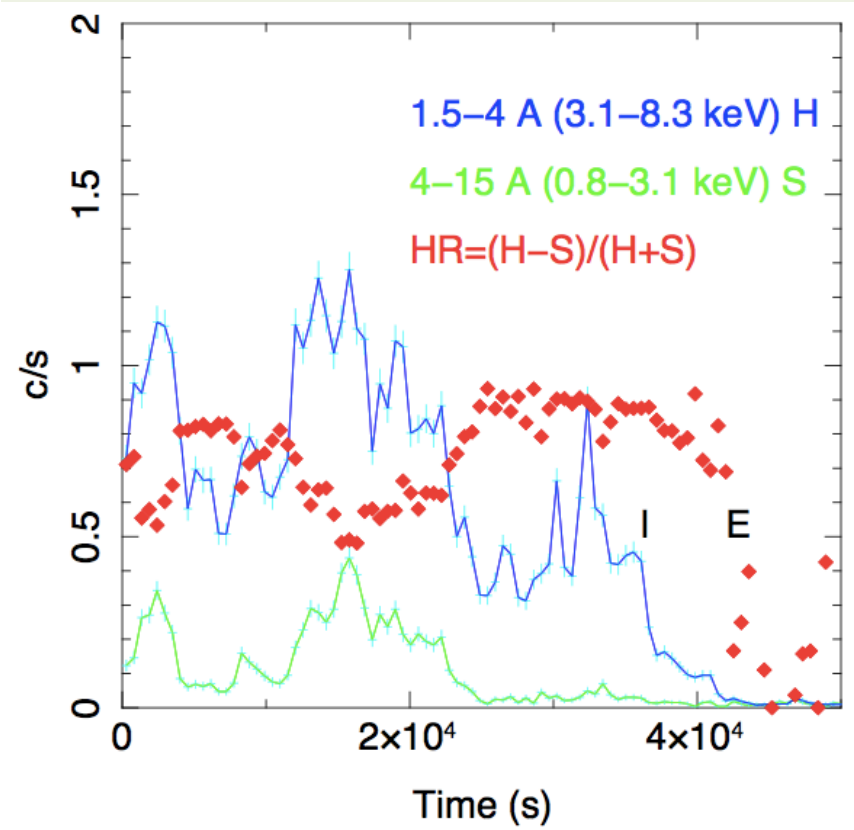

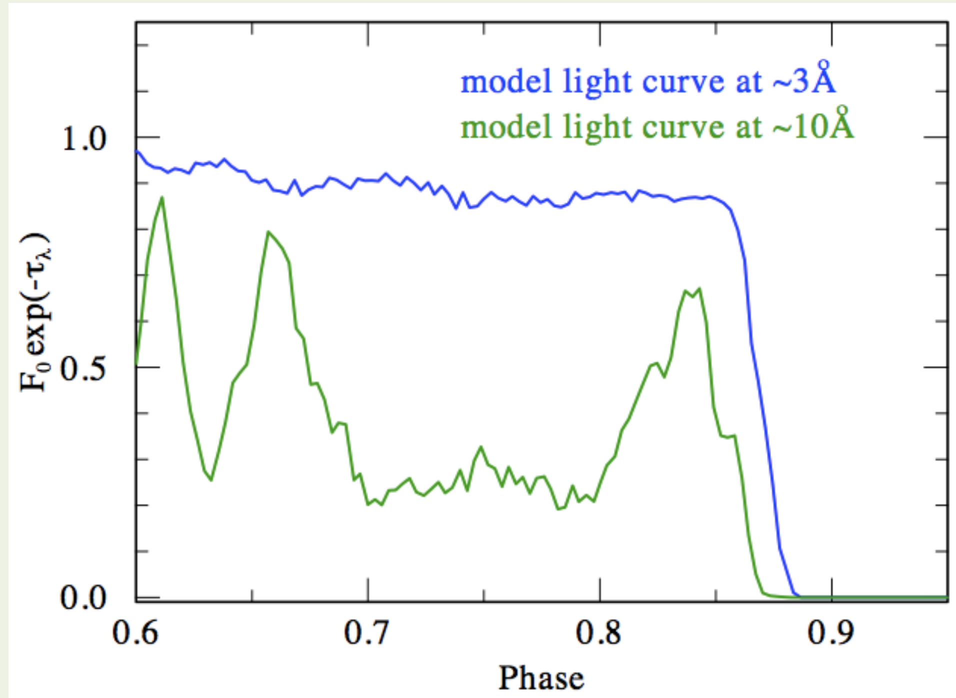

- **Observed** light curve re binned to P_{spin} = 526.69 s
- Strong varibility
- HR anticorrelated with flux

Synthetic light curve:

- Constant X-ray source
- X-rays propagate towards the observed and suffer from absorption in the wind
- Mass-absorption coefficinets from NLTE models κ=20 cm^2 g^{-1} at λ=10 A and κ=3 cm^2 g^{-1} at λ=3 A

HETG Lightcurve

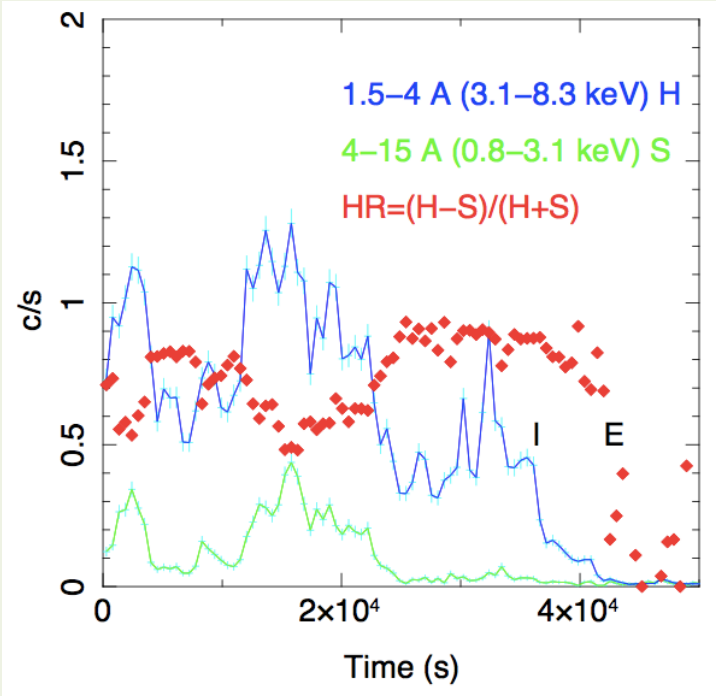

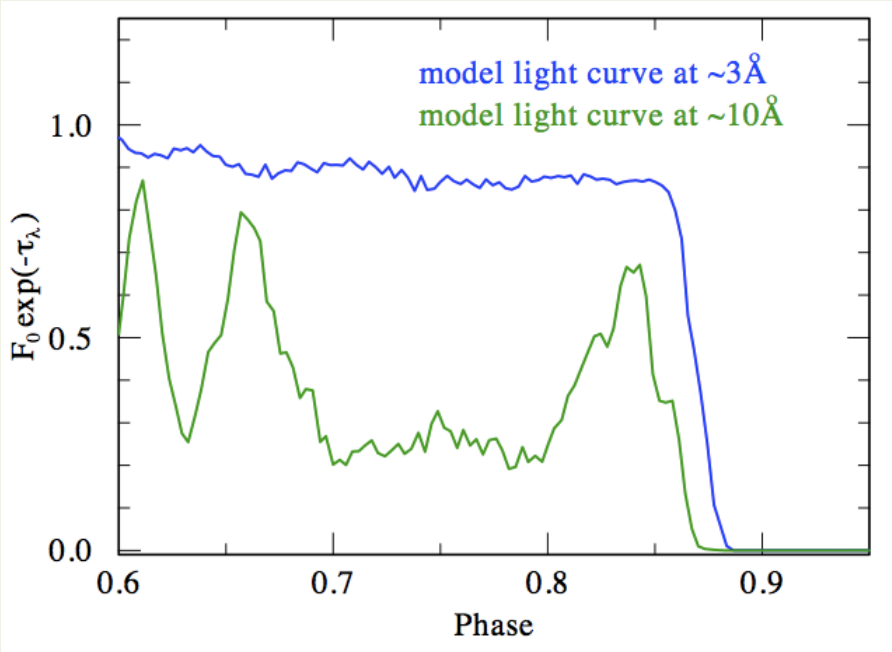

- A **smooth wind** and **stationary accretion** rate can be **excluded**

- The variability observed in the **hard** band can not be explained solely by clump absorption (the wind is transparent for λ < 4 A). There must be **a non-stationary accretion rate**.

- The absorption may help to explain the variability of the **soft** band provided that the **wind is significantly clumped**.

HETG Spectrum: continuum

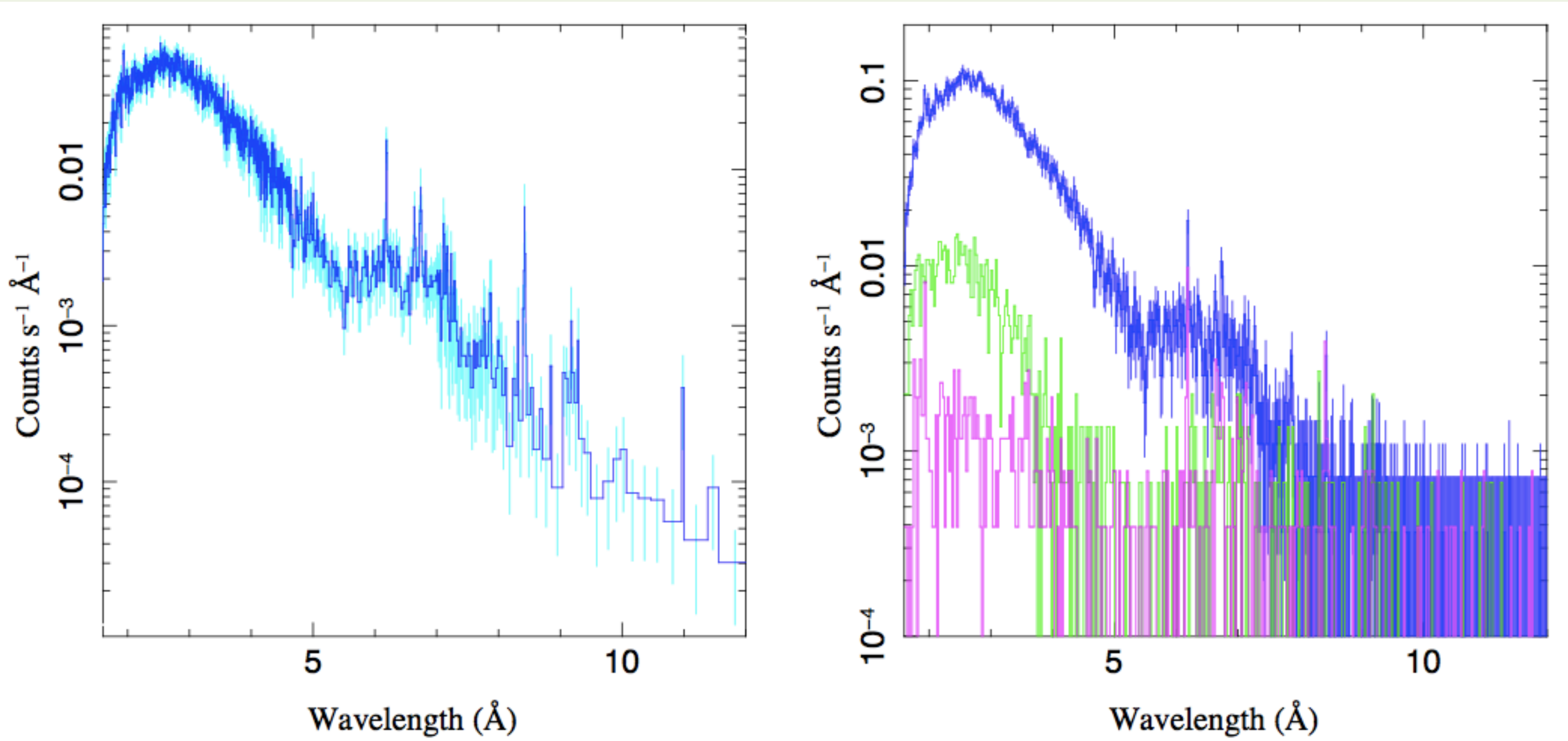

$$F(E) = Abs(E) \times C_{po} \times E^{-\Gamma}$$

HETG Spectrum: continuum

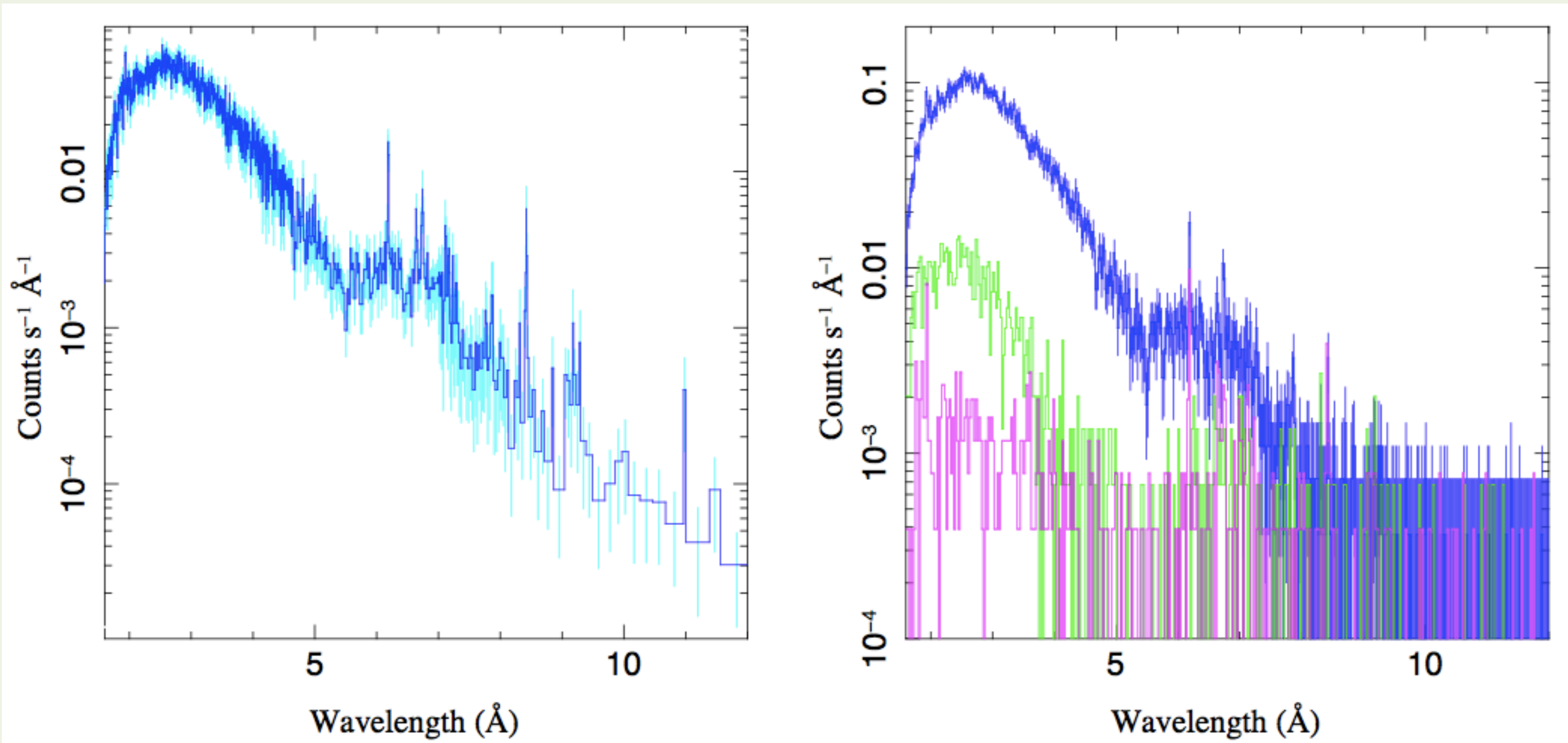

$$Abs(E) = (1-f) * TB_{\mathrm{new}_1}(E) + f * TB_{\mathrm{new}_2}(E)$$

f is the X-ray source *covering fraction* a proxy for the degree of wind clumping.
Tbnew photoelectric absorption (Wilms+ 2010)

Spectrum: continuum model

Model parameters for the continuum.

ϕ	$N_{\rm H}^{1\ (a)}$	$N_{\rm H}^{2}$	f	$C_{po}^{(b)}$	Γ	$N_{\rm H}^{3}$	C_{bb}	kT_{bb}	Flux$^{(c)}$	χ^2_r (dof)
0.77 (O)	$5.1^{+1.1}_{-1.2}$	$12.8^{+1.9}_{-1.4}$	$0.77^{+0.15}_{-0.04}$	$4.5^{+1.3}_{-0.8}$	$1.33^{+0.17}_{-0.15}$	$2.45^{+0.9}_{-0.8}$	$0.3^{+0.1}_{-0.1}$	$0.10^{+0.03}_{-0.02}$	$5.86^{+0.43}_{-0.27}$	0.92 (412)
0.88 (I)	$2.5^{+0.5}_{-0.5}$	$26.1^{+4.4}_{-4.2}$	$0.95^{+0.01}_{-0.05}$	$0.79^{+0.22}_{-0.14}$	1.33 (fixed)	$1.4^{+0.8}_{-0.7}$	$0.2^{+0.1}_{-0.1}$	0.10 (fixed)	$2.51^{+0.23}_{-0.15}$	0.95 (340)
0.97 (E)	$1.6^{+0.9}_{-0.8}$	58^{+10}_{-8}	$0.89^{+0.08}_{-0.09}$	$0.120^{+0.020}_{-0.018}$	1.33 (fixed)	-	-	-	$0.12^{+0.02}_{-0.02}$	0.95 (343)

[a] All $N_{\rm H}$ in units of $\times 10^{22}$ cm^{-2}.
[b] All C in units of $\times 10^{-2}$
[c] Unabsorbed 1-10 keV *model* flux in units of $\times 10^{-10}$ erg s^{-1} cm^{-2}

$$Abs(E) = (1-f) * TB_{\rm new_1}(E) + f * TB_{\rm new_2}(E)$$

$$N_{\rm H}^{1} = N_{\rm H}^{\rm inter-clump} + N_{\rm H}^{\rm ISM}$$

$$N_{\rm H}^{2} = N_{\rm H}^{\rm clumps} + N_{\rm H}^{\rm ISM}$$

Spectrum: continuum model

Model parameters for the continuum.

ϕ	$N_{\rm H}^{1\ (a)}$	$N_{\rm H}^{2}$	f	$C_{po}^{(b)}$	Γ	$N_{\rm H}^{3}$	C_{bb}	kT_{bb}	Flux$^{(c)}$	χ^2_r (dof)
0.77 (O)	$5.1^{+1.1}_{-1.2}$	$12.8^{+1.9}_{-1.4}$	$0.77^{+0.15}_{-0.04}$	$4.5^{+1.3}_{-0.8}$	$1.33^{+0.17}_{-0.15}$	$2.45^{+0.9}_{-0.8}$	$0.3^{+0.1}_{-0.1}$	$0.10^{+0.03}_{-0.02}$	$5.86^{+0.43}_{-0.27}$	0.92 (412)
0.88 (I)	$2.5^{+0.5}_{-0.5}$	$26.1^{+4.4}_{-4.2}$	$0.95^{+0.01}_{-0.05}$	$0.79^{+0.22}_{-0.14}$	1.33 (fixed)	$1.4^{+0.8}_{-0.7}$	$0.2^{+0.1}_{-0.1}$	0.10 (fixed)	$2.51^{+0.23}_{-0.15}$	0.95 (340)
0.97 (E)	$1.6^{+0.9}_{-0.8}$	58^{+10}_{-8}	$0.89^{+0.08}_{-0.09}$	$0.120^{+0.020}_{-0.018}$	1.33 (fixed)	-	-	-	$0.12^{+0.02}_{-0.02}$	0.95 (343)

[a] All $N_{\rm H}$ in units of $\times 10^{22}$ cm^{-2}.
[b] All C in units of $\times 10^{-2}$
[c] Unabsorbed 1-10 keV *model* flux in units of $\times 10^{-10}$ erg s^{-1} cm^{-2}

$E(B\text{-}V)$=2.2 (Crampton+ 1978) → $N^{\rm ISM}_{\rm H} \approx 1.5 \times 10^{22}$ cm^{-2}

$$N_{\rm H}^{1} = N_{\rm H}^{\rm inter-clump} + N_{\rm H}^{\rm ISM}$$

At $\Phi = 0.97$ (E) → $N^{\rm inter\text{-}clump}_{\rm H} \approx 0$

The interclump medium contributes very little to the continuum absorption

We have an "extra" $N_{\rm H}$ ($5.1-1.5 \approx 3.6 \times 10^{22}$ cm^{-2}) at $\Phi = 0.77$

Spectrum: continuum model

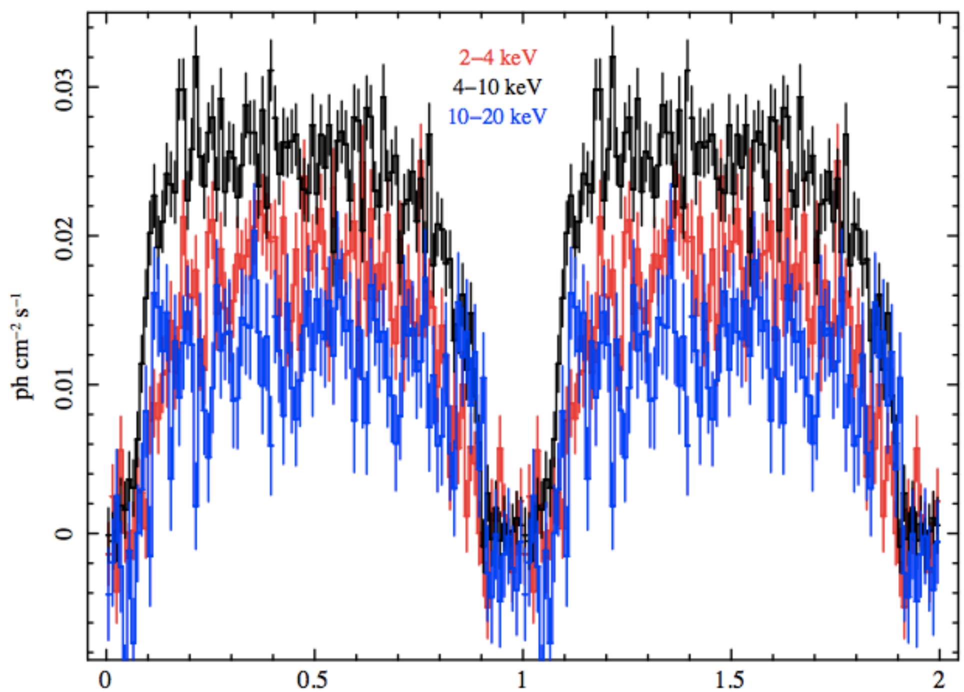

MAXI 5 years lightcurve

(Rodes-Roca+ 2015)

Chandra HETG spectrum consistent with increased absorption in the second half of the orbit.

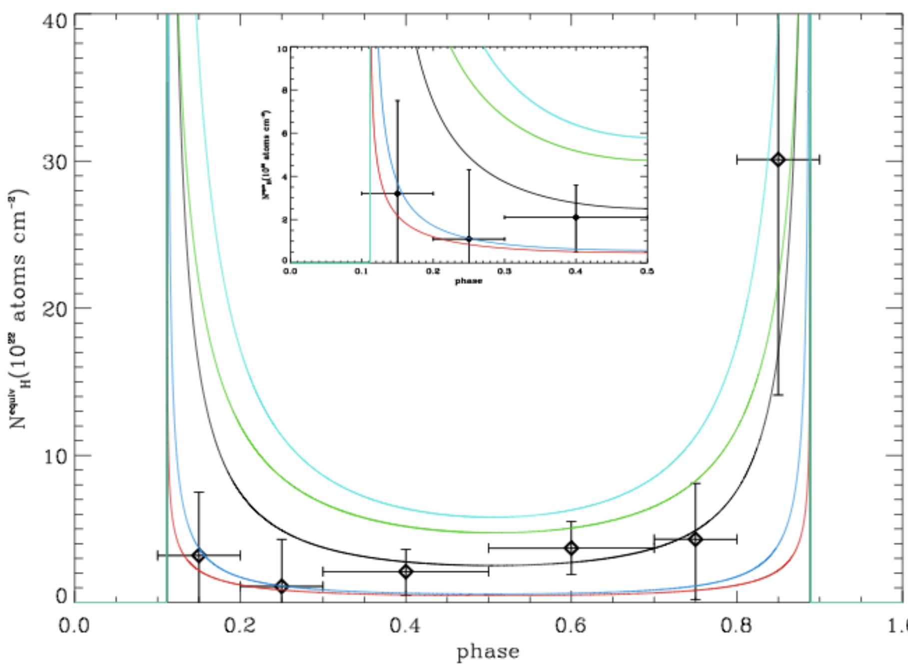

Spectrum: He-like triplets

Emission lines identified in the *Chandra* phase average spectrum of QV Nor

Ion	λ (Å)	Flux $\times 10^{-4}$ (ph s^{-1} cm^{-2})	σ (Å)
Si XIV Lyα	$6.1880^{+0.0019}_{-0.0017}$	$2.2^{+0.08}_{-0.06}$	0.005
Si XIII r	6.6396	$1.8^{+1.0}_{-0.6}$	0.005
Si XIII i	6.6850	<0.75	0.005
Si XIII f	6.7377	$1.8^{+1.0}_{-0.7}$	0.005
Si Kα	$7.1186^{+0.0005}_{-0.0010}$	$1.0^{+1.8}_{-0.5}$	0.005
Mg XII Lyα	8.4236 ± 0.0032	10^{+13}_{-5}	$0.009^{+0.009}_{-0.005}$
Mg XI r	9.1688	1.2 ± 0.7	0.005
Mg XI i	9.2300	< 0.6	0.005
Mg XI f	9.3136	1.5 ± 0.7	0.005

Note. — Numbers without errors are fixed to the quoted value.

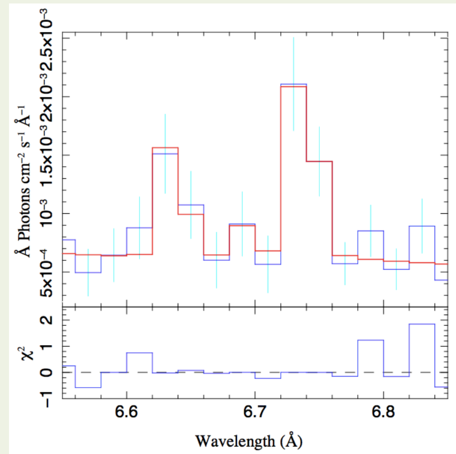

Si XIII (O)

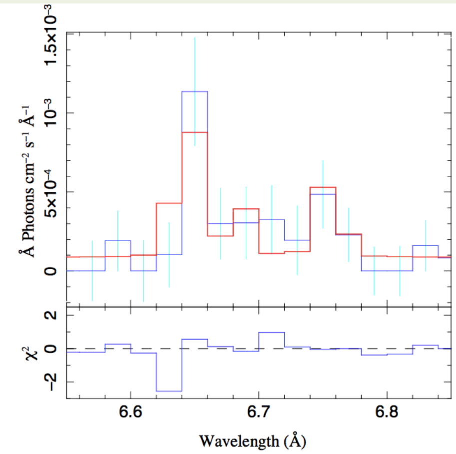

Si XIII (E)

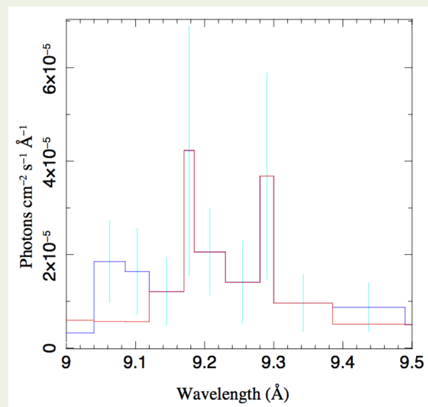

Mg XI

Si XIII He-like triplet

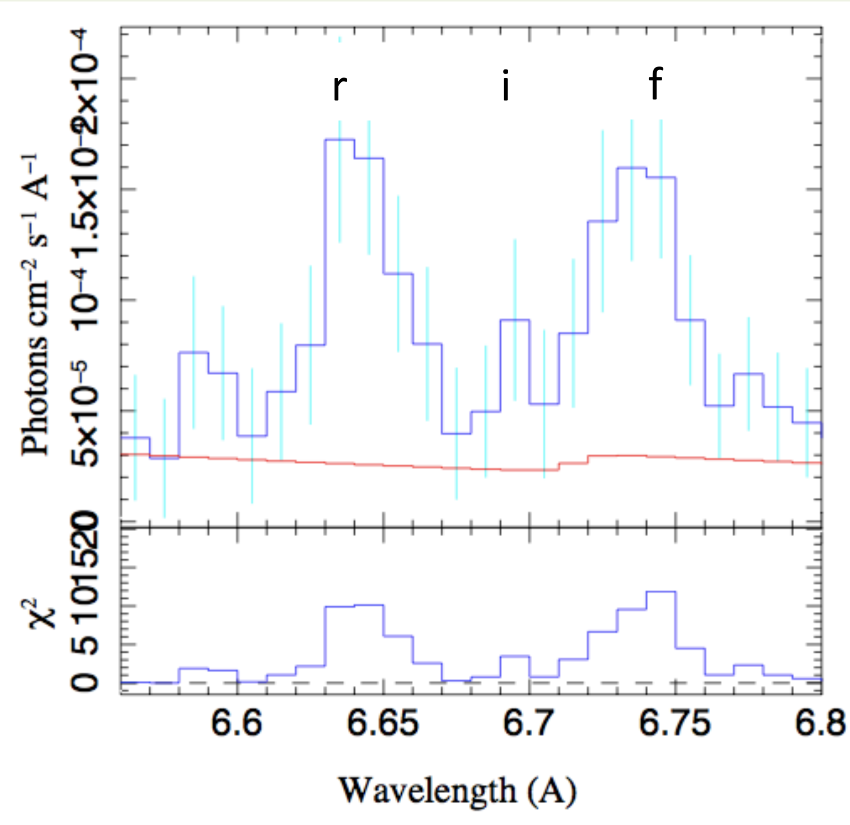

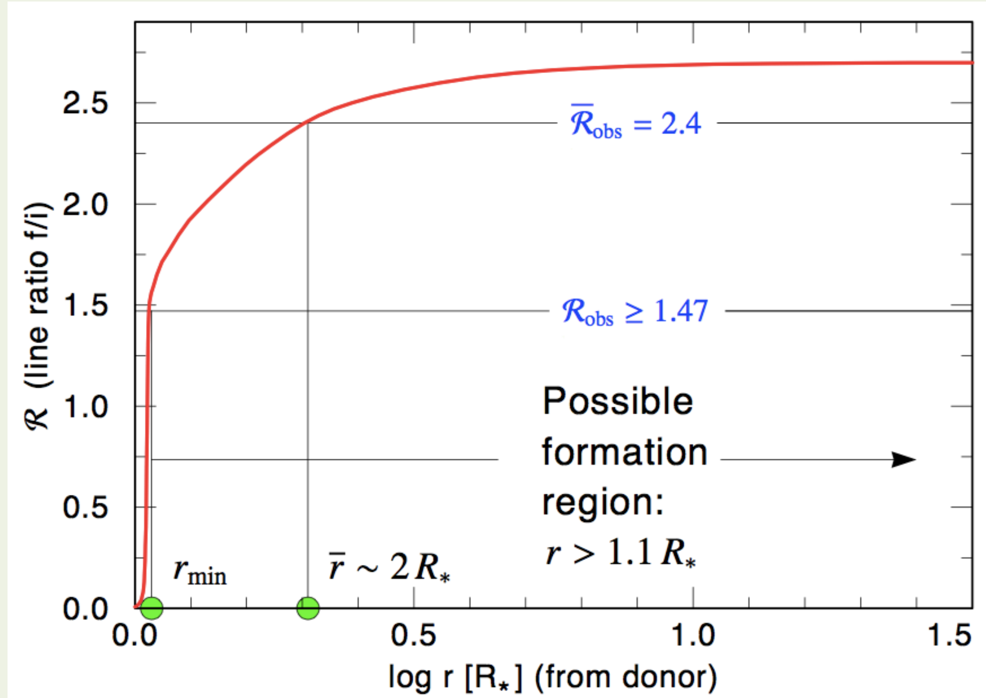

r ≈ f not expected from a photoinozed plasma

i significant (AD test) but very weak

R = f/i the formation region can not be constrained with the available data

The Fe lines

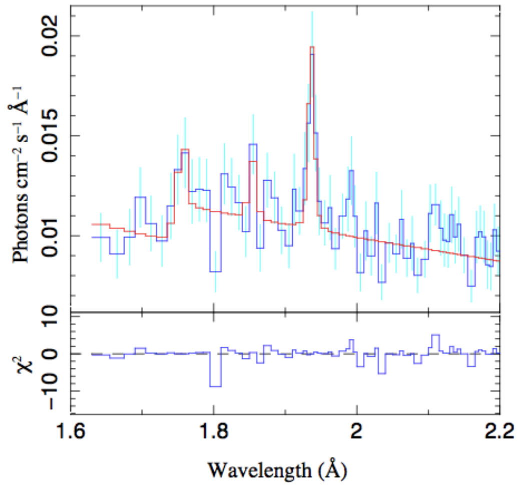

ϕ = 0.77 (O)

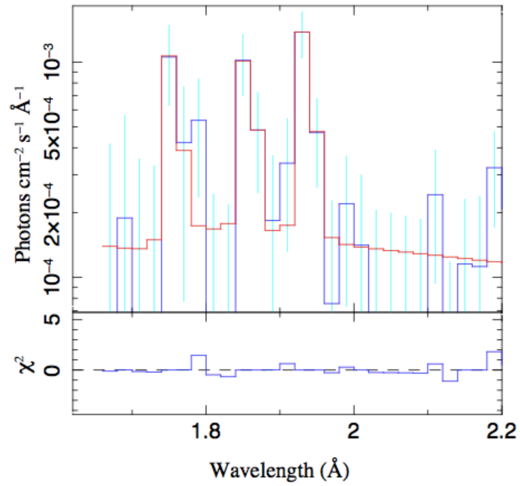

ϕ = 0.97 (E)

Fe emission lines identified in the *Chandra* spectrum of QV Nor at several orbital phases.

Ion	λ (Å)	Flux $\times 10^{-4}$ (ph s^{-1} cm^{-2})	σ (Å)
Out of eclipse			
Fe Kβ	$1.7551^{+0.0035}_{-0.0021}$	$0.5^{+0.1}_{-0.4}$	$\leqslant$0.005
Fe XXV	1.8588$\pm$ 0.0025	$0.5^{+0.4}_{-0.4}$	$\leqslant$0.005
Fe Kα	$1.9368^{+0.0032}_{-0.0018}$	$1.4^{+0.3}_{-0.1}$	$\leqslant$0.005
Eclipse			
Fe Kβ	$1.7551^{+0.0036}_{-0.0021}$	$0.22^{+0.6}_{-0.15}$	0.005
Fe XXV	1.8574$\pm$ 0.0025	$0.3^{+0.7}_{-0.2}$	0.005
Fe Kα	$1.9368^{+0.0035}_{-0.0019}$	0.38$\pm$0.16	0.005

Note. — Numbers without errors are fixed to the quoted value.

The Fe lines

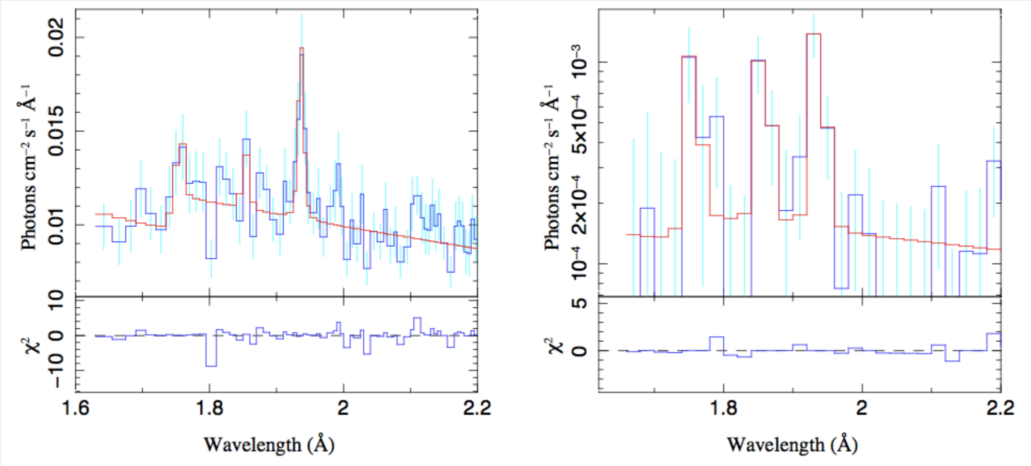

- The Fe Kα λ range is compatible with Fe II-X and the λ centroid with **Fe III-VIII → log ξ = [-1, 2]** (Kallman+ 2004, Fig.5) with a most likely predominance of log ξ < 0

- The **line is narrow, not resolved by *Chandra* HEG** gratings, implying that the bulk of the reprocessing material has $\mathbf{v_w \leq 800}$ **km/s**
- $\boldsymbol{F^{line}_E}$**= 0.3** $\boldsymbol{F^{line}_O}$ (while F^{cont}_E=0.03 F^{cont}_O)

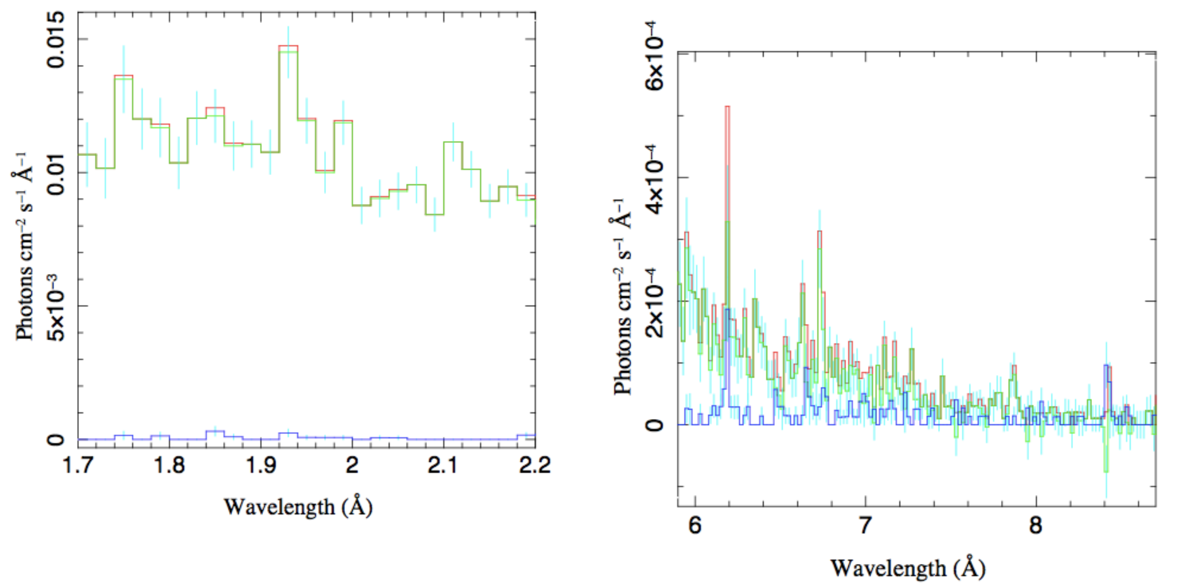

Figure 10. Left: Fe Kα region showing the out-of-eclipse spectrum (red), the eclipse spectrum (blue, barely visible at the bottom of the plot) and the subtracted spectrum (green). As can be seen, the contribution of the eclipse spectrum to the total spectrum is very small. The errors are only show for the eclipse and subtracted spectrum for clarity. Right: 5.9 - 8.7 Å region with the same color code as before.

Fe Kα photons (λ=1.9368 A) can <u>not</u> be resonantly scattered in the wind. Only photons shortward of the Kα edge (λ <1.75 A) have enough energy to effectively excite fluorescence. The observed **Fe Kα emission must come from regions** in the wind **direclty in the line of sight to the observer** and the neutron star simultaneosuly.

70% of the **Fe Kα photons must be produced at distances from the NS r_X < 1R***

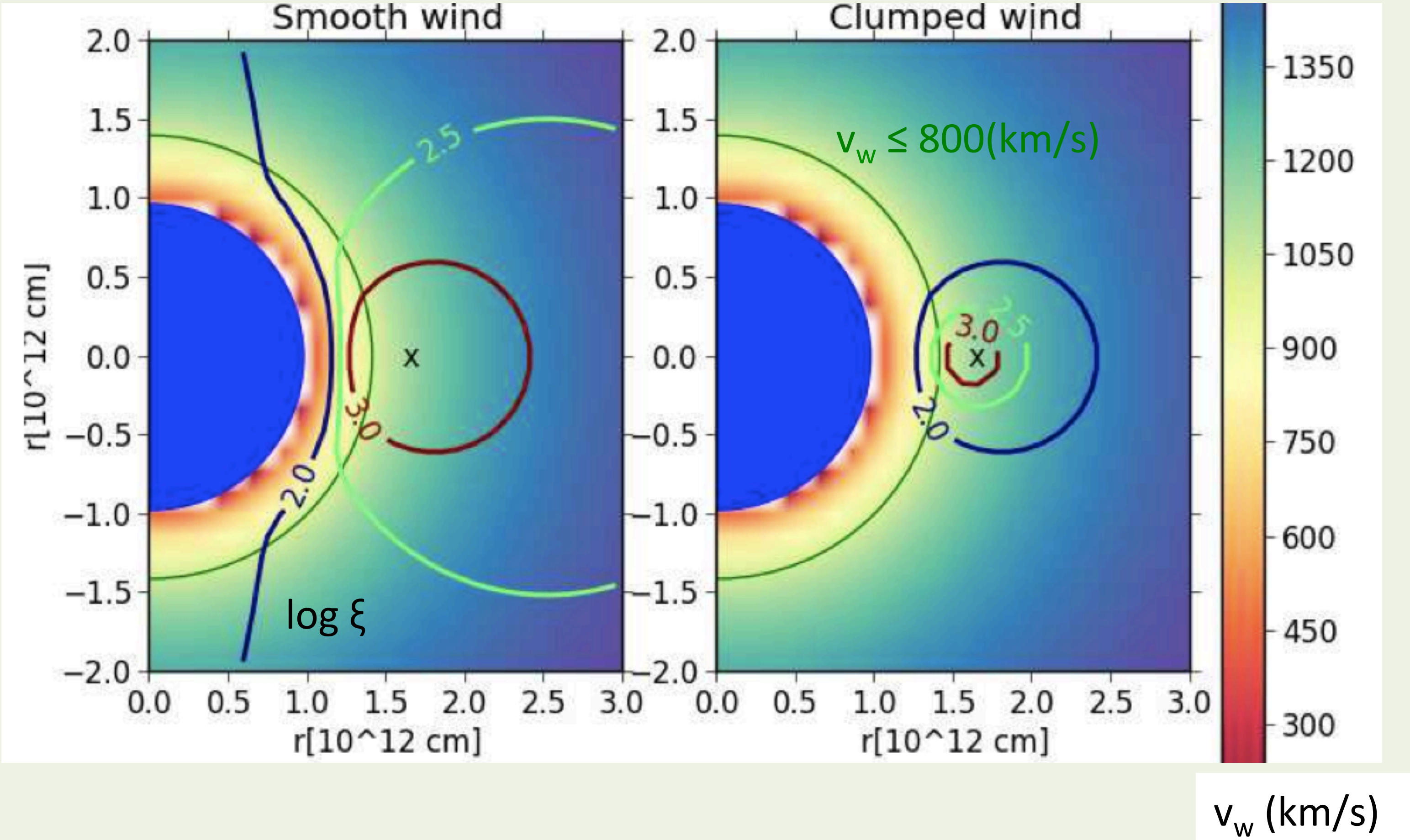

Fe Kα photons must come from the wind region that meet the conditons:

$$v_w \leq 800 \text{ km/s}$$

$$\log \xi \leq 2$$

The vast majority of Fe Kα emission must be produced at radial distances from QV Nor ≤ 1.25 R* in the direction facing the NS

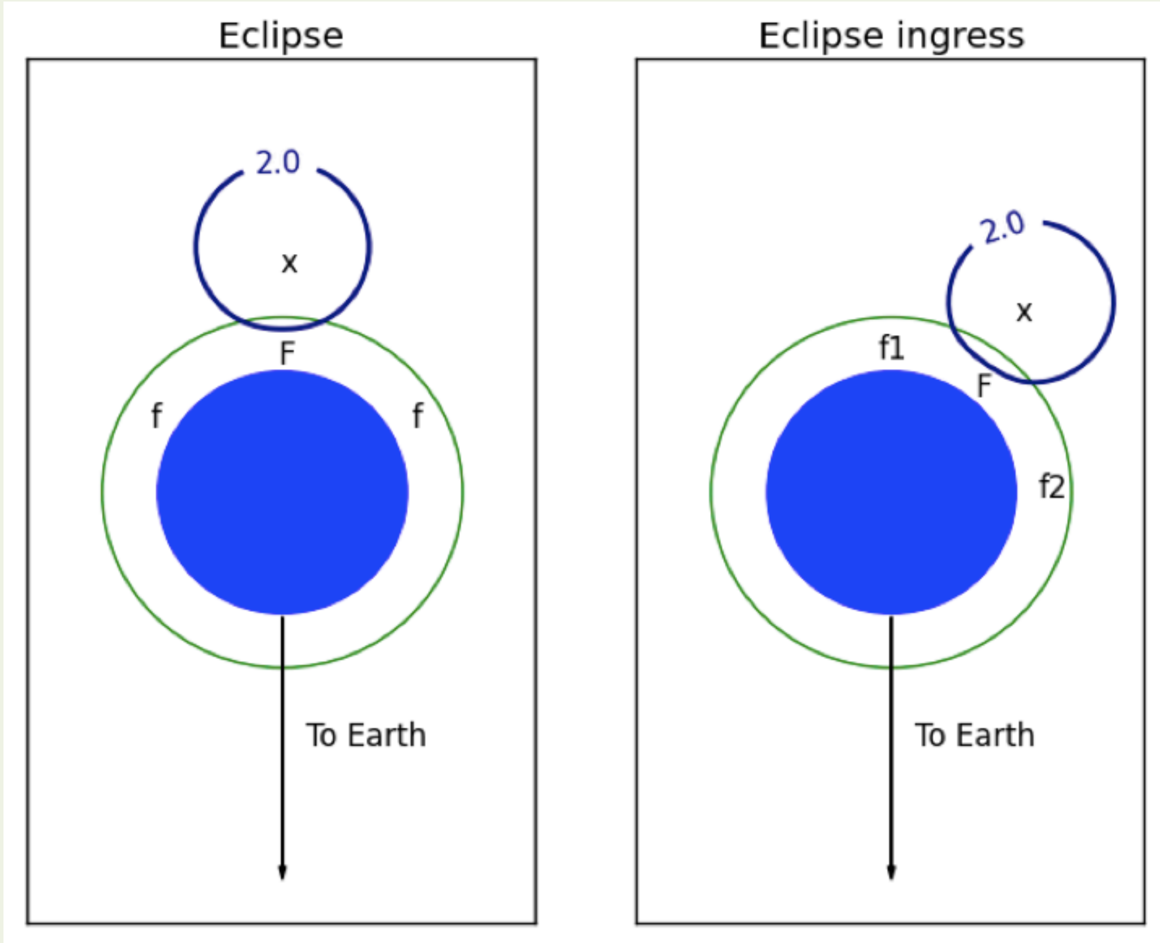

Fe Kα photons must come from the wind region that meet the conditons:

$$v_w \leq 800 \text{ km/s}$$

$$\log \xi \leq 2$$

The vast majority of Fe Kα emission must be produced at radial distances from QV Nor ≤ 1.25 R* in the direction facing the NS

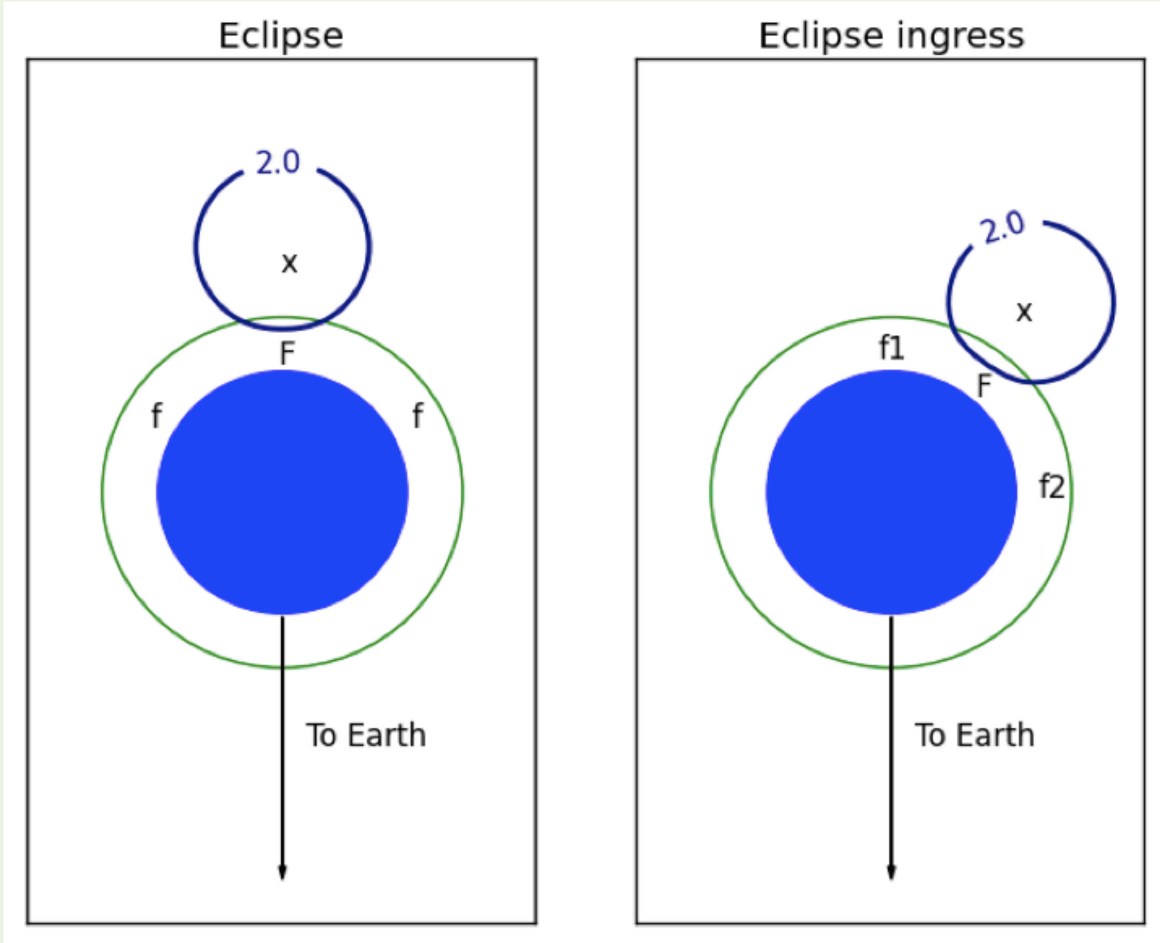

If this scenario is correct we should observe:

a) A *minimum* Fe Kα emission during ingress

b) A *maximum* Fe Kα at orbital phase ϕ = 0.5

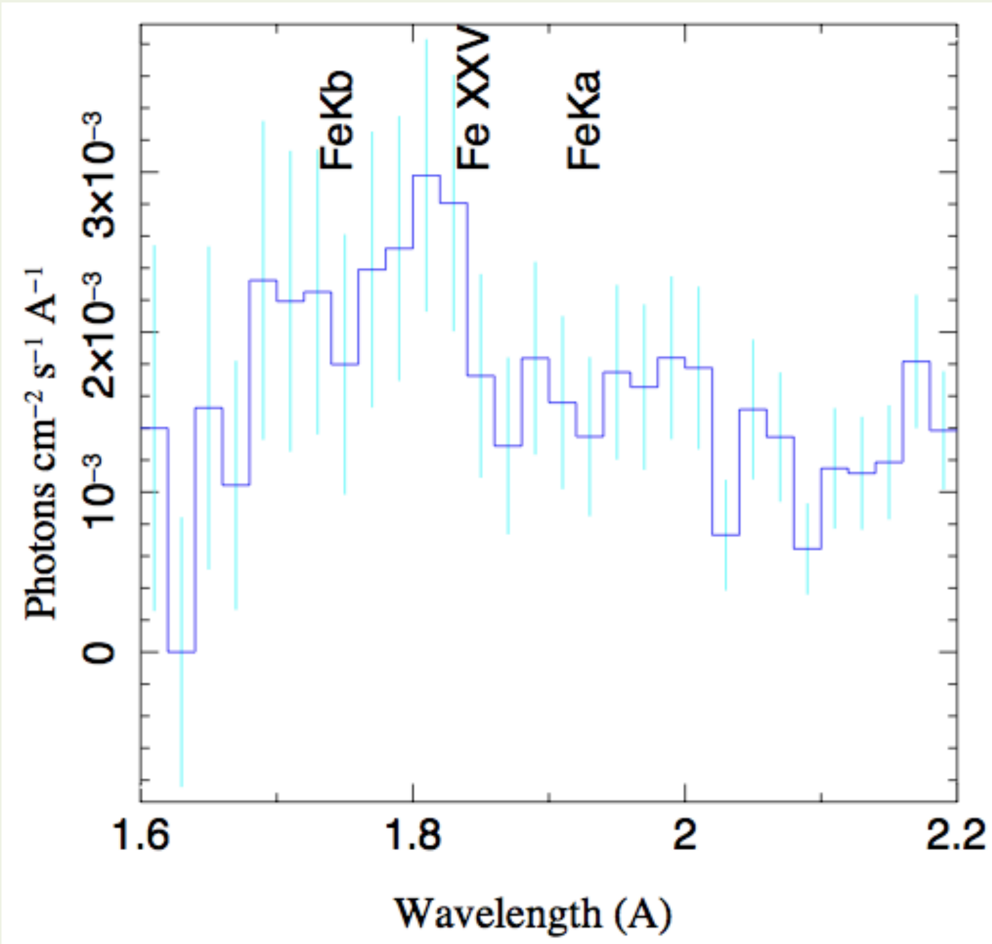

$I_{FeK\alpha}$

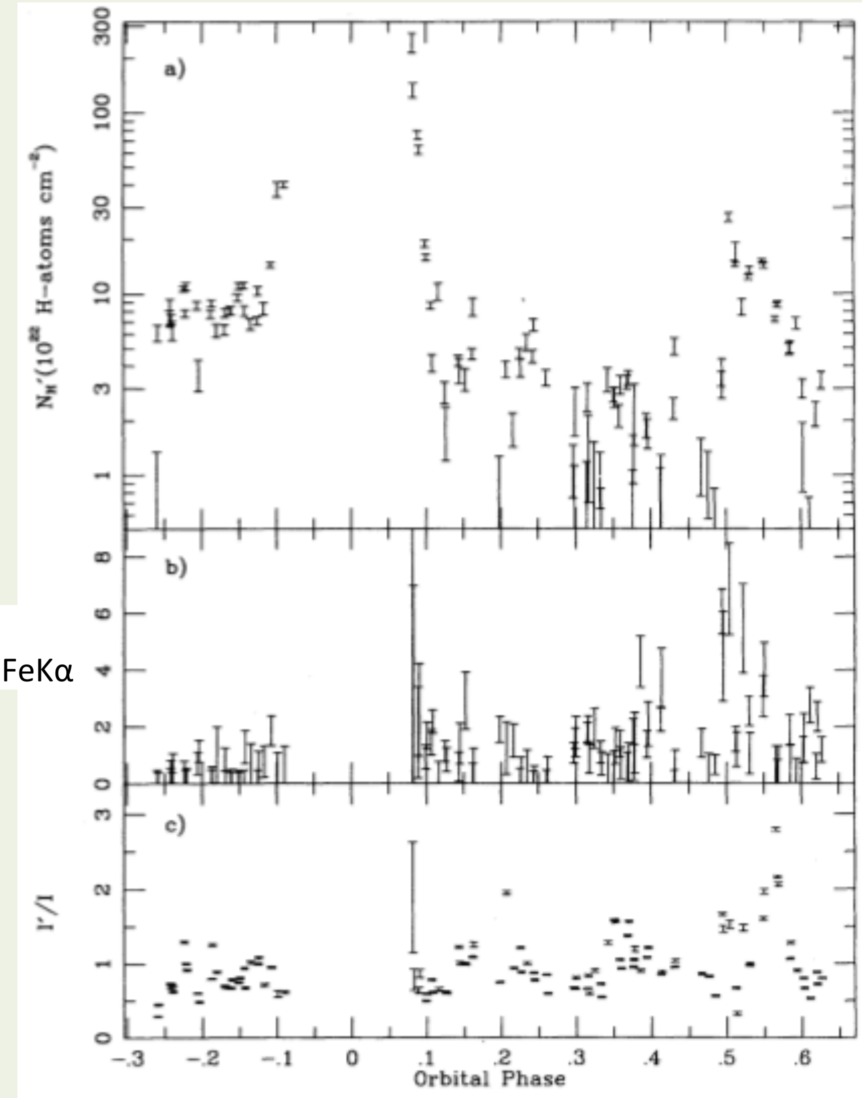

FIG. 2.—Plots of fitted quantities characterizing the X-ray spectra against orbital phase: (*a*) column density of hydrogen atoms; (*b*) iron line intensity; (*c*) intensity fluctuations relative to the synthesized average source spectra.

Ingress (ϕ=0.88)

No FeK lines are seen

Clark+94

Other sites for Fe Kα

Two other places can meet the conditions above:

- **Accretion wake**: the contribution must be minor because it should still be visible in phase bin I when no Fe line is observed.
- **Ionization wake**: the contribution must be minor, as well, because the Fe is near to neutral.

Conclusions

- The Fe Kα emission is mostly confined to the stellar wind region that meets the conditions v_w < 800 km and log ξ < 2, in the direction facing the NS.

- The stellar wind of the B0I star QV Nor must be significantly clumped at $r < 1.25R_*$ (probably an upper limit)

- At such small radial distances, the wind instabilities may not be fully developed and a triggering mechanism should be invoked.

- Subsurface convection can be at work in OB stars (Cantiello & Braithwaite 2011) giving rise to localized surface magnetic fields. These could trigger such instabilities.

- Our *Chadra* observation provides firm empirical evidence of strong inhomogeneity in a B-type star supergiant wind close to stellar photosphere.